Transport mean free path in $K_5Bi_{1-x}Nd_x(MoO_4)_4$ laser crystal powders

2007 J. Phys.: Condens. Matter 19 036206

(http://iopscience.iop.org/0953-8984/19/3/036206)

INSTITUTE OF PHYSICS PUBLISHING JOURNAL OF PHYSICS: CONDENSED MATTER

J. Phys.: Condens. Matter **19** (2007) 036206 (12pp) doi:10.1088/0953-8984/19/3/036206

Transport mean free path in $K_5Bi_{1-x}Nd_x(MoO_4)_4$ laser crystal powders

M A Illarramendi[1], I Aramburu[1], J Fernández[1,2,3], R Balda[1,2,3] and M Al-Saleh[1]

[1] Departamento de Física Aplicada I, Escuela Técnica Superior de Ingeniería, Universidad del País Vasco, Alda. Urquijo s/n, 48013 Bilbao, Spain
[2] Unidad Física de Materiales CSIC-UPV/EHU, 20080 Donostia, Basque Country, Spain
[3] Donostia International Physics Center (DIPC), 20080 Donostia, Basque Country, Spain

E-mail: mariaasuncion.illarramendi@ehu.es

Received 27 June 2006, in final form 24 October 2006
Published 5 January 2007
Online at stacks.iop.org/JPhysCM/19/036206

Abstract

In this work, we calculate in two different ways the transport mean free paths in $K_5Bi_{1-x}Nd_x(MoO_4)_4$ ($x = 0.05, 0.2, 1$) laser crystal powders by using the diffuse spectral reflectance and transmittance of the powders and the absorption coefficient of the crystal materials. The theoretical calculations have been made by assuming a diffusive propagation of light in these materials. Similar results have been obtained from both methods.

1. Introduction

Since the discovery in 1986 of a laser-like behaviour in a powder of $Na_5La_{1-x}Nd_x(MoO_4)_4$ crystallites [1], laser crystal powders (LCPs) have been studied extensively [2–6]. The laser radiation generated in LCPs is described as random lasing with non-resonant feedback. A laser with non-resonant feedback is an extreme case of a multimode laser with very strong interactions between modes. The central emission wavelength of such a laser is determined by the resonant wavelength of a gain medium rather than eigenmodes of the cavity. This type of laser has no spatial coherence, it is not stable in phase, and its photon statistics is strongly different from that of a conventional laser. Consequently, laser crystal powders are attractive as compact and mirrorless lasers where the coherence is not necessary or the absence of coherence is desirable. These characteristics can be advantageous in holography, in laser inertial confinement fusion or in transport of energy in fibres for medical applications [3, 6]. The potential applications of LCPs motivate the study of their optical properties and the search for new crystal powder materials. This is the case of $K_5Bi_{1-x}Nd_x(MoO_4)_4$ disordered crystal powders. Among oxide laser crystals with a disordered structure, palmierite-type $K_5Bi_{1-x}Nd_x(MoO_4)_4$ compounds have generated a great interest as potential laser materials [7–9]. In particular, the authors have reported for the

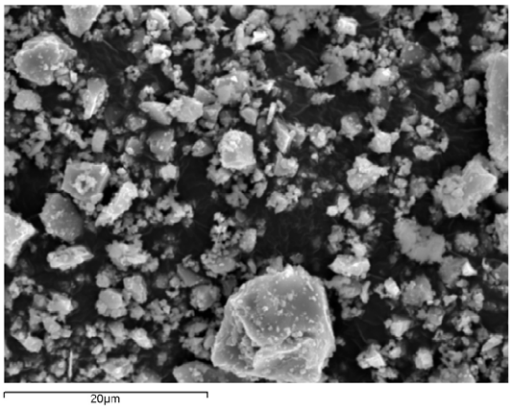

Figure 1. Scanning electron microscope photograph of the stoichiometric laser crystal $K_5Nd(MoO_4)_4$ particles.

first time an experimental demonstration of broadband wavelength self-frequency tuning in $K_5Nd(MoO_4)_4$ laser crystal [10]. The lasing wavelength range of these materials is confined within the 1063–1070 nm region.

In order to better understand the operation regime of random lasers, a detailed characterization of the propagation of pumping and fluorescence light in scattering materials is needed. In particular, the knowledge of the mean free path lengths involved in the scattering and absorption processes that take place in these materials is very important in analysing the behaviour of random lasers. It has been shown that the threshold of random lasers is strongly dependent on the transport mean free path [11–13]. Therefore, the calculation of this parameter is an essential task in the study of random laser materials. In the present work, we have determined the transport mean free path in $K_5Bi_{1-x}Nd_x(MoO_4)_4$ ($x = 0.05, 0.2, 1$) laser crystal powders by using the diffuse reflectance and transmittance of the powders and the absorption coefficient of the crystal materials. The theoretical calculations have been made by assuming a diffusive propagation of light in these materials. The source of diffuse radiation is an incoming coherent beam whose amplitude is exponentially decaying along the sample.

The paper is organized as follows. The experimental techniques are described in section 2. The theoretical analysis of the diffuse reflectance and transmittance of laser crystal powders under a diffusion assumption is given in section 3. In section 4, the transport mean free paths of $K_5Bi_{1-x}Nd_x(MoO_4)_4$ ($x = 0.05, 0.2, 1$) laser crystal powders are calculated in two different ways and the results obtained are discussed. A summary of the work is presented in section 5.

2. Experimental techniques

In our experiments, we have used ground powders of $K_5Bi_{1-x}Nd_x(MoO_4)_4$ ($x = 0.05, 0.2, 1$) laser crystals. Details of the crystallographic structure of the single crystals and their laser properties have been previously reported by the authors [8–10]. The polydispersity of the measured powders was evaluated from SEM (scanning electron microscope) photographs like the one showed in figure 1. The particle size has been computed calculating the mean of the major and minor axis lengths of the grains. As an example, figure 2 shows the histogram of the particle size corresponding to the stoichiometric laser crystal powder $K_5Nd(MoO_4)_4$ (KNM). Fitting the histogram to a log-normal function, we obtain the average particle size and

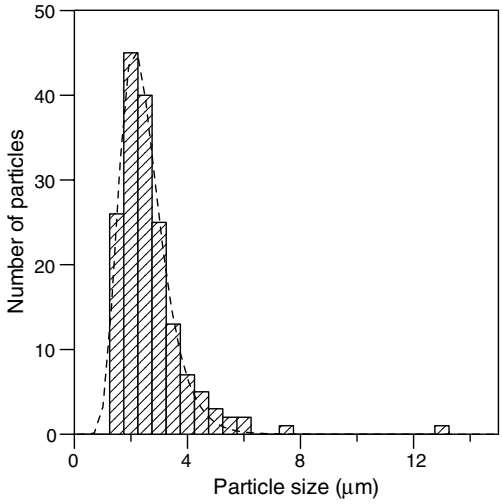

Figure 2. Histogram of the KNM particle size. The dashed line is the log-normal fit from which the average particle size is calculated.

its standard deviation: 2.4 ± 0.8 μm. Similar average particle sizes have been obtained for the other samples. The ratio between the standard deviation and the average particle size gives the polydispersity of the powders, which is around 36% in our samples. The volume filling factor of the powder materials (f) has been calculated by measuring the volume and weight of the samples.

The room-temperature absorption spectra of the single crystals in the 300–800 nm spectral range were recorded by use of a Cary 5 spectrophotometer. The diffuse reflectance spectra of the powders were recorded with an integrated sphere setup. The appropriate normalizations of the recorded spectra have been made to the reflection of the diffused ideally white standard reference sample (Al_2O_3 powder). The thickness of the samples in these measurements was $L = 3$ mm. The transmission measurements of the samples were made by exciting with an Ar laser ($\lambda = 514$ nm) and detecting the transmitted signal at the same wavelength with a Hamamatsu R928 photomultiplier. The signal was amplified by a standard lock-in technique. In the reflectance measurements the volume filling factor of the samples was $f = 0.35 \pm 0.05$, whereas in the transmittance ones $f = 0.60 \pm 0.05$.

3. Theoretical modelling of transmission and reflection

Light propagation through optically dense random systems, where the transport mean free path is much longer than the light wavelength ($l_t \gg \lambda$), is commonly described in terms of a diffusion equation [14–18]. In contrast to the source of diffuse radiation taken in [14–16], where the incident photons are left at a certain plane inside the sample, the source considered in this paper is the extinguished (scattered and absorbed) light of the incoming coherent beam. The intensity of this coherent light decays exponentially along the scattering sample. This source with a spatial extension is closer to the source of a real system, a fact that can be important if we want to analyse the experimental measurements correctly [17, 18].

Let us consider a plane wave incident along the z-direction upon a slab sample which dimensions x and y are much larger than the z-dimension. By assuming that the only source is light incoming from the z-direction, which decays exponentially through the slab

as $J_0 \exp(-\frac{z}{l^*})$, the steady-state diffusion equation applicable to this case is written as [19]

$$\frac{\partial^2 U_d}{\partial z^2} - \frac{U_d}{l_{abs}^2} = -\frac{3J_0}{4\pi l_s}\left[\frac{1}{l_t} + \frac{\bar{\mu}}{l^*}\right]\exp\left(-\frac{z}{l^*}\right) \tag{1}$$

where $U_d(z)$ is the average diffuse intensity, l_{abs} is the diffusive absorption length, J_0 is the incident flux, l_s is the scattering mean free path, and l^* is the extinction mean free path. The definitions of these mean free paths are given in the appendix. $\bar{\mu}$ is the average cosine of the scattering angle (the asymmetry parameter). Equation (1) has been worked out by taking suitable boundary conditions. These have been determined by considering that the diffuse fluxes going from the boundaries inside the sample are due to the internal reflectivities at the sample surfaces (r). The transmittance T of the slab has been calculated by the sum of the incoming flux and the diffuse flux evaluated at the sample surface $z = L$ and normalized by the incident flux (J_0), whereas the diffuse reflectance R is due to the normalized diffuse flux evaluated at the sample surface $z = 0$. The obtained expressions for these magnitudes are written as

$$T = \frac{a + b\exp(-L/l^*)\cosh(L/l_{abs}) + c\exp(-L/l^*)\sinh(L/l_{abs})}{d\cosh(L/l_{abs}) + e\sinh(L/l_{abs})} \tag{2}$$

$$R = \frac{f\exp(-L/l^*) + f\cosh(L/l_{abs}) + g\sinh(L/l_{abs})}{d\cosh(L/l_{abs}) + e\sinh(L/l_{abs})}. \tag{3}$$

a, b, c, d, e, f and g are functions which depend on the mean free paths, the asymmetry parameter, and the internal average reflectivities at the sample surfaces. L is the thickness of the scattering sample. The complete expressions of these functions are given in the appendix of this paper.

At large values of L ($L \gg l_{abs}$) the transmittance decays exponentially with thickness as $T \sim \exp(-\frac{L}{l_{abs}})$, whereas the reflectance does not depend on sample thickness, and it can be described in the form

$$R = \{(3l_{abs}(3l_{abs}l_i(l_i - 2hl_s + 3\bar{\mu}l_s + l_s) - 6h\bar{\mu}l_{abs}(l_i + l_s)l_t + l_i((2h(l_i + 3\bar{\mu}l_s + l_s) - 3\bar{\mu}(l_i + l_s))l_t - 3l_il_s))))\}\{(((l_i + l_s)^2l_t - 3l_il_s^2)(3l_i + 4h(3l_{abs} + hl_t)))\}^{-1} \tag{4}$$

where $h = \frac{1+r}{1-r}$, and l_i the inelastic mean free path, which is defined as the length of the light path in which intensity is reduced to 1/e of its initial value due only to absorption. This last expression for reflectance can be rewritten as [20]

$$\mathrm{Ln}(-\mathrm{Ln}R) = \mathrm{Ln}\alpha + \beta \cdot \mathrm{Ln}\left(\frac{1}{l_i}\right) \tag{5}$$

where α is a parameter which depends on the scattering mean free path l_s, the anisotropy parameter $\bar{\mu}$, and the internal reflectivity r. β is a dimensionless parameter and in addition to the dependence with $l_s, \bar{\mu}, r$, it also depends on the inelastic mean free path l_i. In the limit of very low absorption ($l_i \to \infty$), the β parameter tends to 0.5. Equation (5) allows us to analyse the variation of diffuse reflectance with l_i, that is, with absorption. The analytical general expressions of α ($l_s, \bar{\mu}, h$) and β ($l_s, \bar{\mu}, h, l_i$) parameters are given in [20].

4. Results and discussion

Figure 3 shows the measurements used to obtain the experimental dependence of the diffuse reflectance with absorption. Figure 3(a) shows the absorption spectrum averaged over different polarizations in the 350–750 nm wavelength range for $K_5Bi_{1-x}Nd_x(MoO_4)_4$ ($x = 0.05, 0.2, 1$)

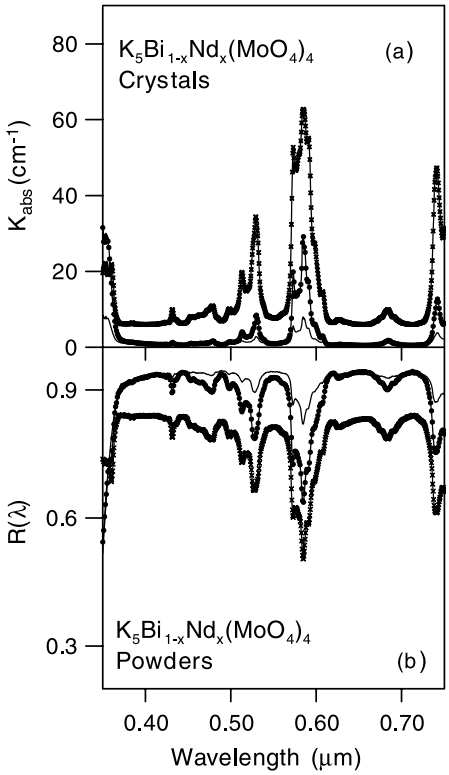

Figure 3. (a) Absorption spectrum of $K_5Bi_{1-x}Nd_x(MoO_4)_4$ ($x = 0.05$, 0.2, 1) laser crystals averaged over different polarizations. (b) Spectral reflectance of $K_5Bi_{1-x}Nd_x(MoO_4)_4$ ($x = 0.05$, 0.2, 1) powders. The reflection spectrum of the powders has been recorded using an integrated sphere. The single solid line corresponds to the sample with $x = 0.05$, the solid line with dots corresponds to the sample with $x = 0.2$ and the solid line with crosses to the stoichiometric powder ($x = 1$). The same nomenclature has been used in both sections of the figure. The volume filling factor of the powder materials in these measurements is $f = 0.35 \pm 0.05$.

single crystals. In figure 3(b) the spectral diffuse reflectances of the corresponding crystal powders have been plotted. These results correspond to absolute measurements. It must be noticed that in the spectral regions where the neodymium ion Nd^{3+} presents very low absorption, the reflectance values of the stoichiometric sample (KNM) are displaced from reflectance values of the other samples. This effect can be due to a decrease of the optical quality of the crystal samples as the concentration of Nd^{3+} is increased. Figure 4 represents $\mathrm{Ln}(-\mathrm{Ln}(R(\lambda)))$ as a function of $\mathrm{Ln}(1/l_i(\lambda))$ for KNM and $K_5Bi_{0.8}Nd_{0.2}(MoO_4)_4$ samples in the 560–750 nm wavelength range. The inelastic mean free paths $l_i(\lambda)$ of the compounds have been estimated from the absorption coefficients of the crystal samples [20]. In this calculation, the randomly oriented nonspherical particles have been replaced by area-equivalent spheres and it has been considered that between two successive scattering events the photon experiences an absorption length l_i only inside the particle. From the figure it can be seen that the dependences are approximately linear and therefore the β parameter can be considered constant in that wavelength range. A fitting to equation (5) of the experimental points plotted in figure 4 gives the values $\mathrm{Ln}\alpha = 1.93 \pm 0.05$ and $\beta = 0.483 \pm 0.002$ for KNM powder and $\mathrm{Ln}\alpha = 2.08 \pm 0.03$ and $\beta = 0.491 \pm 0.003$ for the $K_5Bi_{0.8}Nd_{0.2}(MoO_4)_4$ sample. The coefficient of determination

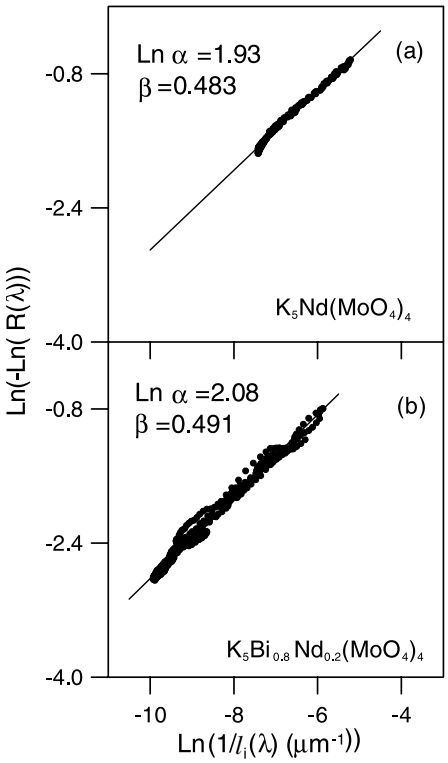

Figure 4. (a) $\mathrm{Ln}(-\mathrm{Ln}(R(\lambda))$ of $K_5Nd(MoO_4)_4$ powder as a function of $\mathrm{Ln}(1/l_i(\lambda)))$. The solid circles represent the experimental points and the solid line is the linear fitting. (b) $\mathrm{Ln}(-\mathrm{Ln}(R(\lambda))$ of $K_5Bi_{1-x}Nd_x(MoO_4)_4$ ($x = 0.2$) powder as a function of $\mathrm{Ln}(1/l_i(\lambda)))$. The solid circles represent the experimental points and the solid line is the linear fitting. The coefficient of determination (R^2) of both linear fittings is 0.99.

(R^2) of the linear fitting is 0.99 in both cases. The linear fitting of $\mathrm{Ln}(-\mathrm{Ln}(R(\lambda))$ versus $\mathrm{Ln}(1/l_i l_i(\lambda))$ for the sample with lowest concentration of Nd^{3+} ($x = 0.05$) is worse than the other ones, $R^2 = 0.91$, and the values obtained are $\mathrm{Ln}\alpha = 1.96 \pm 0.07$ and $\beta = 0.497 \pm 0.007$. This can be due to the low values of the absorption coefficient in this sample that would produce a greater dispersion of experimental points. It must be noticed that as the Nd^{3+} concentration decreases, that is, the absorption diminishes, the value of the slope β increases from 0.483 to 0.497. This agrees with the theory because the β value tends to 0.5 in the limit of very low absorption.

Once the values of α and β have been determined, we can calculate the average values of the transport mean free path for our crystal powders in that wavelength range by using the analytical expressions of $\alpha(l_s, \bar{\mu}, h)$ and $\beta(l_s, \bar{\mu}, h, l_i)$. The average internal reflectivity of the samples has been estimated from the Fresnel reflection coefficients $R(\theta)$ by means of the expression [21]

$$\bar{r} = \frac{3R_2 + 2R_1}{3R_2 - 2R_1 + 2} \qquad \text{with } R_1 = \int_0^{\frac{\pi}{2}} R(\theta) \cos\theta \sin\theta \, \mathrm{d}\theta$$
$$\text{and } R_2 = \int_0^{\frac{\pi}{2}} R(\theta) \, (\cos\theta)^2 \sin\theta \, \mathrm{d}\theta. \tag{6}$$

Fresnel reflection coefficients have been calculated by taking as the effective refractive index

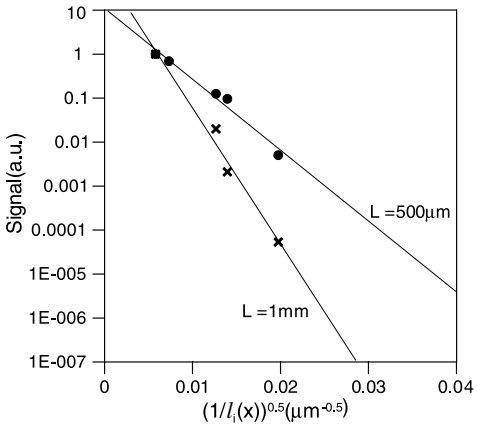

Figure 5. Transmittance of $K_5Bi_{1-x}Nd_x(MoO_4)_4$ ($x = 0$, 0.01, 0.05, 0.1, 0.2) powders at $\lambda = 514$ nm as a function of $(1/l_i(x))^{0.5}$. The symbols represent the experimental points and the solid line is the linear fitting. The volume filling factor of the powder materials in these measurements is $f = 0.60 \pm 0.05$.

Table 1. Transport mean free paths in microns of $K_5Bi_{1-x}Nd_x(MoO_4)_4$ ($x = 0.05$, 0.2, 1) powders determined by different methods. The values in parentheses in the last row correspond to the values of l_t obtained with the assumption of independent scattering.

Method	Range (nm)	l_t (μm) $K_5Bi_{1-x}Nd_x(MoO_4)_4$ $x = 0.05$	l_t (μm) $K_5Bi_{1-x}Nd_x(MoO_4)_4$ $x = 0.2$	l_t (μm) $K_5Nd(MoO_4)_4$ $x = 1$
$\mathrm{Ln}(-\mathrm{Ln}R(\lambda))$ versus $\mathrm{Ln}(1/l_i(\lambda))$ $f = 0.35$	560–750	7.5 ± 1.9	5.9 ± 0.9	5.8 ± 0.9
$T(\frac{1}{\sqrt{l_i}})$ $f = 0.60$	514	5.5 ± 1.0	5.5 ± 1.0	5.5 ± 1.0
Mie theory Averaged size $= 2.4$ μm $f = 0.35$	514	6.11 (5.97)	6.11 (5.97)	6.08 (5.96)

of the random system the Maxwell–Garnet effective refractive index ($n \cong 1.23$ for $f = 0.35$). By solving the equations $\mathrm{Ln}\alpha = $ constant and $\beta = $ constant numerically, with the conditions $0 \leqslant \bar{\mu} \leqslant 1$ and $\lambda \leqslant l_s \leqslant L$, we have obtained values of l_t for all samples, which are displayed in table 1. The estimated relative error for the values corresponding to samples with $x = 0.2$ and 1 is 15%, while the error for the sample with $x = 0.05$ is higher, 25%.

On the other hand, we have analysed the dependence of diffuse transmittance with absorption by measuring the transmittance of several samples with different concentrations of Nd^{3+} ion (x) at fixed sample thickness. Figure 5 shows in logarithmic scale the diffuse transmittance as a function of $(1/l_i(x))^{0.5}$ for two different thicknesses, and confirms the exponential dependence of transmittance, valid at $L \gg l_{abs}$ (see section 3). The first point of the figure corresponds to $K_5Bi(MoO_4)_4$ ($x = 0$) sample, which presents a large value of l_i. In this case, l_{abs} (around 200 μm) is comparable with the sample thickness and the exponential dependence of transmittance could not be satisfied. However, the experimental results suggest that, in practice, the applicability range of the exponential dependence of transmittance can

be extended from $L \gg l_{abs}$ to $L \sim l_{abs}$. Due to the low absorption at $\lambda = 514$ nm, the value of l_t is practically the same in the studied samples ($x = 0$, 0.01, 0.05, 0.1, 0.2), so the fitting of the experimental points to the exponential, $\exp(-L/l_{abs}) = \exp(-L/\sqrt{\frac{l_t l_i}{3}})$, gives the value of the transport mean free path for these powders directly. The values of l_t obtained are 5.2 ± 0.9 μm for $L = 500$ μm and 5.9 ± 1.1 μm for $L = 1$ mm. The mean value of $l_t = 5.5 \pm 1$ μm has been displayed in table 1. Since the volume filling factor f of the samples used in $R(\lambda)$ measurements ($f = 0.35$) is lower than the f of the samples used in transmittance method ($f = 0.6$), it is expected that the l_t values obtained using the first method should be higher. However, this effect can be counteracted by the fact that the wavelength used in the transmittance method is lower than wavelength range corresponding to the first method. Moreover, samples with a volume filling factor $f = 0.6$ are closely-packed powders and spatial correlations among scatterers could smooth the variation of transport mean free paths with volume filling factor [22]. Therefore, we can say that the agreement between the l_t values obtained from the two methods is very good. These values of l_t for $K_5Bi_{1-x}Nd_x(MoO_4)_4$ are comparable to the values experimentally determined by other techniques in other similar laser crystal powders [20, 23].

Finally, we have calculated the photon mean free paths by applying Mie theory and compared them with the previous values experimentally obtained. Due to the fact that volume fractions occupied by the powders are high, the photon mean free paths have been calculated from the scattering and transport Mie cross-sections with spatial correlations among scatterers, σ_s^c and σ_t^c:

$$l_s^c = \frac{1}{\rho\sigma_s^c} \qquad \text{with } \sigma_s^c = \int \frac{d\sigma}{d\Omega} S(\theta)\, d\Omega \tag{7}$$

$$l_t^c = \frac{1}{\rho\sigma_t^c} \qquad \text{with } \sigma_t^c = \int \frac{d\sigma}{d\Omega} (1 - \mathrm{Cos}\,\theta) S(\theta)\, d\Omega. \tag{8}$$

In these expressions, ρ is the number density of scatterers and $\frac{d\sigma}{d\Omega}$ is the differential scattering cross-section [24]. $S(\theta)$ is the static structure factor which accounts for particle correlations and it has been calculated by using the Percus–Yevick approximation for hard spheres [25, 26]. Although the values of the absorption cross-section in the whole wavelength range are much lower than the values of the scattering cross-section, they have been taken into account in the calculations. The determination of the cross-sections has been done with the following assumptions. (i) The randomly oriented nonspherical particles have been replaced by area-equivalent spheres. Due to the relatively large value of the size parameter ($x = 2\pi r/\lambda$) for these compounds ($x \sim$ 10–20), the nonspherical–spherical differences are expected to be small [27]. (ii) The broad size distribution of particles has been substituted by spheres with the diameter equal to the averaged mean particle size. The cross-sections and the asymmetry parameters of the particles have been averaged over a radius interval $\Delta r \sim \lambda/2$ (or $\Delta x \sim \pi$) which is enough for the ripple structure to vanish [28]. It can be shown that these mean free paths differ by only ~5% from those calculated with the averaged mean particle size. The values obtained for l_t at 514 nm for each sample are in agreement with those obtained experimentally and they have been added to table 1. From beginning to end of the 560–750 nm wavelength range, the value of the transport mean free path only changes by 12%, which lies within the estimated error for l_t. This is due to the fact that the absorption cross-sections of the powders in the wavelength range studied (350–800 nm) are very small if compared with the values of the scattering cross-sections. As a result, the effect of the absorption on the transport mean free paths is insignificant and their variation through the wavelength range is mainly due to the variation of the size parameter. This can be the reason why the averaged l_t obtained from the reflectance method is in agreement with the value of l_t obtained from the transmittance one at

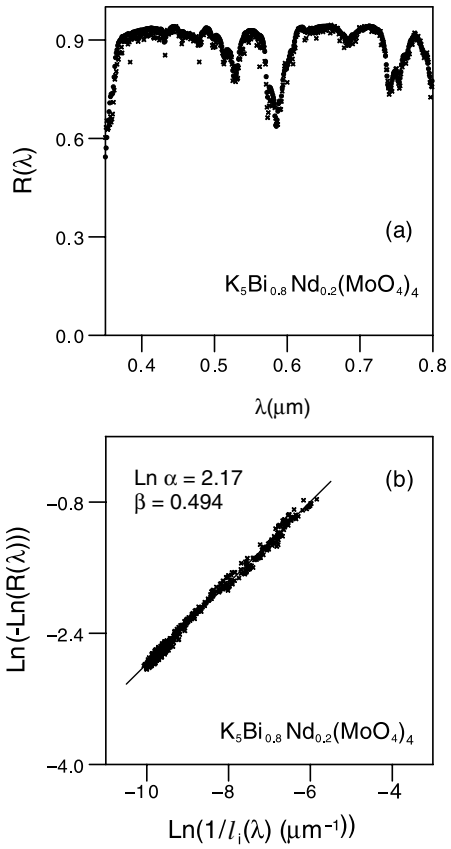

Figure 6. (a) Spectral reflectance $R(\lambda)$ of $K_5Bi_{1-x}Nd_x(MoO_4)_4$ ($x = 0.2$) powder. The crosses are the theoretical curve while the dots are the experimental curve. The theoretical $R(\lambda)$ curve has been calculated from the wavelength dependence of the complex refractive index of $K_5Bi_{0.8}Nd_{0.2}(MoO_4)_4$ material with an averaged particle size equal to 2.4 μm and a volume filling factor $f = 0.35$. (b) $\mathrm{Ln}(-\mathrm{Ln}(R(\lambda))$ as a function of $\mathrm{Ln}(1/l_i(\lambda))$ for the previous theoretical spectral reflectance $R(\lambda)$. The solid crosses represent the points calculated from Mie theory and the solid line is the linear fitting.

$\lambda = 514$ nm. A good agreement is also obtained between experimental and theoretical spectral diffuse reflectance. Figure 6(a) shows the experimental and the theoretical spectral diffuse reflectance of $K_5Bi_{0.8}Nd_{0.2}(MoO_4)_4$ laser crystal powder in the 350–800 nm wavelength range. The theoretically calculated spectrum $R(\lambda)$ has been obtained by determining the wavelength dependence of all mean free paths from Mie theory and introducing them into equation (4). In figure 6(b) $\mathrm{Ln}(-\mathrm{Ln}(R(\lambda))$ has been plotted as a function of $\mathrm{Ln}(1/l_i(\lambda))$ for the theoretically calculated $R(\lambda)$ in the 560–750 nm wavelength range. The values of α and β calculated from the theoretical dependence entirely agree with those obtained experimentally (see figure 4(b)).

It can be verified that if scattering were considered to be independent, that is, each particle is in the far-field zones of all the other particles and the scattering by individual particles is incoherent, the results obtained would not basically change (see the values in parentheses in table 1). As an example, we have calculated the ratios between the scattering and transport mean free paths with and without correlation, l_s^c/l_s and l_t^c/l_t, for $K_5Nd(MoO_4)_4$ material at $\lambda = 0.514$ μm for an averaged particle size of 2.4 μm. Figure 7 shows those ratios as a

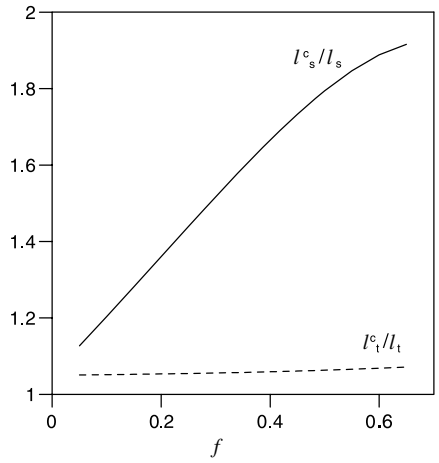

Figure 7. Ratios l^c_s/l_s (solid line) and l^c_t/l_t (dashed line) versus volume fraction of the scatterers for an averaged particle size of 2.4 μm. The data correspond to $K_5Nd(MoO_4)_4$ powder at $\lambda = 514$ nm. The values of l^c_s/l_s and l^c_t/l_t at $f = 0.6$ are 1.89 and 1.05, respectively.

function of the volume fraction occupied by the scatterers. It can be seen that l^c_s/l_s increases with increasing f while $l^c_t \simeq l_t$ is satisfied independently of the f value, which indicates that spatial correlations have a stronger effect on the scattering mean free paths than on the transport mean free paths. As a result, we can say that the values of the transport mean free path are not modified by the inclusion of the spatial correlations and the small variation in the scattering mean free paths does not alter the experimental results (reflectance curves and transmittance data).

5. Summary

The transport mean free paths in $K_5Bi_{1-x}Nd_x(MoO_4)_4$ ($x = 0.05, 0.2, 1$) laser crystals powders have been experimentally determined by using two different techniques. In the first one, the variation with absorption of the spectral diffuse reflectance has been used. In the second one, use has been made of the absorption dependence of the diffuse transmittance for differently doped compounds at fixed sample thickness and at fixed wavelength. A good agreement has been achieved between the results obtained from both methods and those predicted from the Mie theory with spatial correlations.

Acknowledgments

This work was supported by the Spanish Government MEC (MAT2004-03780) and Basque Country University (UPV13525/2001). The authors would like to thank Dr M A Ángeles Laguna (Servicio de Microscopía Electrónica, Universidad de Zaragoza (Spain)) for obtaining the scanning electron microscope photographs.

Appendix

The expressions for the functions $a, b, c, d, e, f,$ and g corresponding to the general expressions of diffuse transmittance and reflectance (equations (2) and (3)) are

$$a = l_i^2 \frac{l_t}{l_{abs}}[3l_i l_s + (3\bar{\mu}(l_i + l_s) + 2h(l_i + 3\bar{\mu}l_s + l_s))l_t] \tag{A.1}$$

$$b = l_i \frac{l_t}{l_{abs}}[-3l_i l_s(l_i + 4hl_s) + (-3\bar{\mu}l_i(l_i + l_s) + 2h(l_i^2 - 3(\bar{\mu} - 1)l_i l_s + 2l_s^2))l_t] \tag{A.2}$$

$$c = (-9l_i^2 l_s^2 - 3l_i l_s((2h + 3\bar{\mu} - 1)l_i + (4h^2 - 1)l_s)l_t + 2h(l_i + l_s)(2h(l_i + l_s) - 3\bar{\mu}l_i)l_t^2) \tag{A.3}$$

$$d = 12hl_{abs}((l_i + l_s)^2 l_t - 3l_i l_s^2) \tag{A.4}$$

$$e = ((l_i + l_s)^2 l_t - 3l_i l_s^2)(4l_t h^2 + 3l_i) \tag{A.5}$$

$$f = 3l_{abs}[l_i(-3l_i l_s + (-3\bar{\mu}(l_i + l_s) + 2h(l_i + 3\bar{\mu}l_s + l_s))l_t)] \tag{A.6}$$

$$g = 9l_{abs}^2[l_i(l_i - 2hl_s + 3\bar{\mu}l_s + l_s) - 2h\bar{\mu}l_t(l_i + l_s)]. \tag{A.7}$$

The *scattering mean free path*, l_s, is the length of the light path in which intensity is reduced to $1/e$ of its initial value due to scattering. It is also defined as the average distance between two successive scattering events. The *transport mean free path*, l_t, is defined as the average distance the light travels before its direction of propagation is randomized. The *inelastic mean free path*, l_i, is the length of the light path in which intensity is reduced to $1/e$ of its initial value due to absorption. The *diffusive absorption length*, l_{abs}, is defined as the average distance between the beginning and the end points of paths of length l_i, $l_{abs} = \sqrt{\frac{l_t l_i}{3}}$. l^* is the *extinction mean free path*, $l^* = (\frac{1}{l_i} + \frac{1}{l_s})^{-1}$, $\bar{\mu} = \langle \cos\theta \rangle$ is the average cosine of the scattering angle (or asymmetry parameter) and $h = \frac{1+r}{1-r}$, where r is the average internal reflectivity.

References

[1] Markushev V M, Zolin V F and Briskina C M 1986 *Sov. J. Quantum. Electron.* **16** 281
[2] Wiersma D S and Lagendijk A 1996 *Phys. Rev.* E **54** 4254
[3] Gouedard C, Husson D, Sautert C, Auzel F and Mignus A 1993 *J. Opt. Soc. Am.* B **10** 2358
[4] Noginov M A, Noginova N E, Caulfield H J, Venkateswarlu P, Thompson T, Mahdi M and Ostroumov V 1996 *J. Opt. Soc. Am.* B **13** 2024
[5] Noginov M A, Noginova N E, Egarievwe S, Caulfield H J, Cochrane C, Wang J C, Kokta M R and Paitz J 1998 *Opt. Mater.* **10** 297
[6] Noginov M A 2005 *Solid-State Random Lasers* (New York: Optical Sciences Springer)
[7] Kaminskii A A, Sarkisov S E, Bohm J, Reiche P, Schultze D and Uecker R 1977 *Phys. Status Solidi* a **43** 71
[8] Voda M, Iparraguirre I, Fernández J, Balda R, Al-Saleh M, Mendioroz A, Lobera G, Cano M, Sanz M and Azkargorta J 2001 *Opt. Mater.* **16** 227
[9] Iparraguirre I, Balda R, Voda M, Al-Saleh M and Fernández J 2002 *J. Opt. Soc. Am.* B **19** 2911
[10] Fernández J, Iparraguirre I, Aramburu I, Illarramendi M A, Azkargorta J, Voda M and Balda R 2003 *Opt. Lett.* **28** 1341
[11] Noginov M A, Zhu G, Frantz A A, Novak J, Williams S N and Fowlkes I 2004 *J. Opt. Soc. Am.* B **21** 191
[12] Totsuka K, Soest G S, Ito T, Lagendijk A and Tomita M 2000 *J. Appl. Phys.* **87** 7623
[13] Ling Y, Cao H, Burin A L, Ratner M A, Liu X and Chang R P 2001 *Phys. Rev.* A **64** 063808
[14] Genack A Z and Drake J M 1990 *Europhys. Lett.* **11** 331
[15] Garcia N, Genack A Z and Lisyansky A A 1992 *Phys. Rev.* B **46** 14475
[16] Gomez-Rivas J, Sprik R, Soukoulis C M, Busch K and Lagendijk A 1999 *Europhys. Lett.* **48** 22
[17] Gomez-Rivas J, Sprik R, Lagendijk A, Noordam L D and Rella C W 2001 *Phys. Rev.* E **63** 046613
[18] Lemieux P A, Vera M U and Durian D J 1998 *Phys. Rev.* E **57** 4498
[19] Ishimaru A 1997 *Wave Propagation and Scattering in Random Media* (New York: IEEE)
[20] Illarramendi M A, Aramburu I, Fernández J, Balda R and Noginov M A 2005 *Opt. Mater.* **27** 1686
[21] Zhu J X, Pine D J and Weitz D A 1991 *Phys. Rev.* A **44** 3948
[22] Saulnier P M, Zinkin M P and Watson G H 1990 *Phys. Rev.* B **42** 2621
[23] Bahoura M and Noginov M A 2003 *J. Opt. Soc. Am.* B **20** 2389
[24] Van de Hulst H C 1981 *Light Scattering by Small Particles* (New York: Dover)

[25] Ashcroft N W and Lekner J 1966 *Phys. Rev.* **145** 83–90
[26] Percus J K and Yevick G Y 1958 *Phys. Rev.* **110** 1–13
[27] Mishchenko M I, Travis L D and Lacis A A 2002 *Scattering, Absorption and Emission of Light by Small Particles* (Cambridge: Cambridge University Press)
[28] Bohren C F and Huffman D R 1983 *Absorption and Scattering of Light by Small Particles* (New York: Wiley)